American Mineralogist, Volume 92, pages 1601–1609, 2007

Fluorophlogopite from Biancavilla (Mt. Etna, Sicily, Italy): Crystal structure and crystal chemistry of a new F-dominant analog of phlogopite

ANTONIO GIANFAGNA,[1] FERNANDO SCORDARI,[2,*] SIMONA MAZZIOTTI-TAGLIANI,[1] GENNARO VENTRUTI,[2] AND LUISA OTTOLINI[3]

[1]Dipartimento di Scienze della Terra—Sapienza Università di Roma, Piazzale Aldo Moro 5, I-00185 Roma, Italy
[2]Dipartimento Geomineralogico—Università degli Studi di Bari, Via E. Orabona 4, I-70125 Bari, Italy
[3]CNR-Istituto di Geoscienze e Georisorse (IGG), Sezione di Pavia, Via Ferrata 1, I-27100 Pavia, Italy

ABSTRACT

Fluorophlogopite, a new F-dominant mineral of the mica group, was found at Monte Calvario, Biancavilla, lower southwestern flanks of Mt. Etna volcano (Catania, Sicily, Italy). The mineral occurs in autoclasts of gray-red altered benmoreitic lavas, primarily associated with fluoro-edenite, alkali-feldspars, clino- and ortho-pyroxenes, fluorapatite, hematite, and pseudobrookite. It was formed by metasomatism of the original lava rocks from very hot fluid enriched in F, Cl, and other incompatible elements. Fluorophlogopite occurs as very thin laminae with a diameter of 200 to 400 μm. Main physical properties are pale yellow in color; yellowish-white in thin section; vitreous to resinous luster; transparent; non-fluorescent; Mohs' hardness 2–3; brittle and malleable; perfect cleavage on {001}; biaxial (–), α_{calc} = 1.5430(8), β = 1.5682(5), γ = 1.5688(5) (λ = 589 nm); $2V_{meas}$ = 17(2)°; α = acute bisectrix ⊥ (001); nonpleochroic; D_{calc} = 2.830 g/cm^3 (using empirical formula and single-crystal unit-cell parameters), D_{calc} = 2.842 g/cm^3 (using empirical formula and powder cell constants). Infrared spectrum did not show a significant absorption band in the OH-stretching region (3800–3600 cm^{-1}) confirming that the F content of the fluorophlogopite from Biancavilla is close to the stoichiometric value.

Unit-cell parameters from X-ray powder-diffraction data (114.6 mm diameter Gandolfi camera, Cu$K\alpha$) are a = 5.305(2), b = 9.189(3), c = 10.137(4) Å, β = 100.02(3)°. These data agree with those obtained by single-crystal X-ray studies on a very thin (~15 μm) fluorophlogopite crystal, i.e., Monoclinic (1M polytype); Space Group $C2/m$; a = 5.3094(4), b = 9.1933(7), c = 10.1437(8) Å, β = 100.062(5)°, V = 487.51(6) Å^3, Z = 2. Structure refinements using anisotropic displacement parameters converged at R = 3.50, R_w = 4.37, R_{sym} = 3.72%. Electron microprobe analysis performed on the same crystal used for X-ray investigation gave: SiO_2 = 45.75(39), TiO_2 = 1.05(5), Al_2O_3 = 9.60(19), MgO = 27.92(30), MnO = 0.16(3), FeO_{tot} = 1.25(6), BaO = 0.09(5), K_2O = 8.22(11), Na_2O = 0.61(30), Cl = 0.02(1) wt%. Secondary Ion Mass Spectrometry (SIMS) was used to estimate light elements [Li_2O = 0.30(1) and H_2O = 0.16(2) wt%] and fluorine content [F = 8.69(24) wt%]. The new mineral fluorophlogopite and its name were approved by IMA-CNMMN (2006/011).

Keywords: Fluorophlogopite, new mineral, crystal chemistry, IR spectroscopy, SIMS

INTRODUCTION

Fluorine is present in the phyllosilicate mineral group in general and in the micas particularly as a substitute for OH. The effects of F-OH replacement on the structure stability have attracted the attention of many researchers (Munoz 1984; Robert et al. 1993; Papin et al. 1997; Mason 1992; Boukili et al. 2001; Fechtelkord et al. 2003). It is well known that the presence of F enhances the thermal stability of the trioctahedral mica structure. The extent of fluorine substitution for OH groups depends on several factors (Boukili et al. 2002 and reference therein). The most important are (1) hydrofluoric acid activity in the fluid during the crystallization and post-crystallization phase; (2) temperature; and (3) cation population of octahedral sheet. Robert et al. (1993), Papin et al. (1997), and Boukili et al. (2001) showed that F exhibits a strong preference for trioctahedral micas because in dioctahedral micas the hydroxyl proton is involved in hydrogen bonds with underbonded apical O atoms from the adjacent tetrahedral sheet, so the replacement of hydroxyl groups by F is difficult or impossible. On the contrary, in trioctahedral micas this replacement does not change significantly the local charge balance on tetrahedral O atoms; in addition the H^+-K^+ repulsion is transformed into F^--K^+ attraction, and therefore it is energetically favored. Boukili et al. (2002) analyzed the relationship between cations distribution over octahedral sites and F content, concluding that F-OH substitution is governed in micas by the structural adaptation of tetrahedral and octahedral layers, not by Al-F or Fe-F bond strength.

As concerns the fluorine end-member of the join (OH,F)-phlogopite (i.e., fluorophlogopite, according to this study),

* E-mail: f.scordari@geomin.uniba.it

literature work refers to synthetic fluorophlogopites because of its applications to material science, as analytical standards, and for several applications in experimental petrology. In this direction, Hammouda et al. (1995) presented a method for synthesizing fluorophlogopite single crystals, suited to laboratory uses, starting from a 1 atm batch melt having a slight excess of F added as K_2SiF_6 and operating in discontinuous cooling conditions. Takeda and Donnay (1966) investigated the structural features of a synthetic lithium fluormica. The structure showed little ditrigonality ($\alpha = 6.22°$) and flattening of octahedral sheet ($\psi = 59.32°$). Joswig (1972) studied by neutron diffraction the crystal structure of a natural F-rich [1.13 F apfu] 1*M*-phlogopite, showing a nearly hexagonal symmetry of the tetrahedral sheet. McCauley et al. (1973) performed a structure refinement on a synthetic fluorophlogopite single crystal from the same batch previously analyzed by Bloss et al. (1963) using powder diffraction technique. The crystal examined by photographic Weissenberg and precession data showed undesirable diffuse streaks and faint extra spots, due respectively to stacking faults and twinning. The smaller twin element was estimated from photographic intensity data to be only about 5% of the total crystal. Hazen and Burnham (1973) reported a single-crystal structure study of a natural phlogopite from the marbles of Franklin, New Jersey with a high-F content [1.30 F apfu]. Takeda and Morosin (1975) determined the unit-cell parameters of a synthetic fluorophlogopite as a function of temperature up to 700 °C. They used the experimental thermal expansivities to calculate some structural parameters to be compared with the observed ones from the structure investigation at 700 °C. Toraya et al. (1978, 1983) studied two synthetic fluoromicas with an excess of Si in the unit formula [Si >> 3 apfu]. They found low ($\alpha = 3.63°$) and very low ($\alpha = 1.73°$) tetrahedral rotation angle inversely related to Al tetrahedral content. Petersen et al. (1982) discussed the frequent incorporation of fluorine in micas and amphiboles, and reported one analysis of a near end-member fluorophlogopite with 1.91 apfu of F found in metamorphosed Adirondack marbles from Balmat, New York. In that work, hydrogen was not directly determined and, apart from unit-cell parameters, no structural study was performed. According to Petersen et al. (1982), fluorine-rich micas may be more present than is evident in the literature because in the past F was not routinely analyzed. The high degree of solid solution between OH and F qualifies the end-member compounds as peculiar phases, which of course have to be considered as independent minerals. Accordingly, they proposed for these particular micas (and also for amphiboles having a high degree of fluorine) a formal list of mineral names, which includes "fluorophlogopite." Unfortunately they were not able to provide evidence concerning its crystal structure. Russell and Guggenheim (1999) refined the crystal structure of a OH-rich 1*M*-phlogopites up to 600 °C, and studied at room temperature and after heat-treatment at 904 °C the crystal structure of a F-rich [0.90 F apfu] 1*M*-phlogopites. They were able to show that OH-rich octahedra expand without changing shape, while F-rich octahedra become elongated approximately along **c** axis. Recently, the F-dominant analog of annite, $KFe^{2+}_3AlSi_3O_{10}(OH)_2$, from the Western Suburb of Suzhou City, near Shangai, China, has been approved by the IMA-CNMMN (99-048) as a new mineral with the name fluorannite (Shen et al. 2000). More recently Xu et al. (2005) pointed out the discovery of a natural F-rich phlogopite from the Bayan Obo ore deposit of Inner Mongolia, China.

The fluorophlogopite under study, from now on labeled F_{nat} (natural fluorophlogopite), has been found for the first time at Biancavilla near Catania (Sicily, Italy), on the southwest flank of the Etnean Volcanic Complex, during a mineralogical and environmental study of that area (Gianfagna et al. 2003; Comba et al. 2003), because of the presence of fibrous fluoro-edenite amphiboles. Natural fluoro-edenite, a new mineral (IMA-CNMMN 2000-49), was found for the first time at Biancavilla (Gianfagna and Oberti 2001). The fluorophlogopite and the fluoro-edenite occur in the same volcanic products constituted by altered benmoreitic lavas.

The discovery of a natural fluorophlogopite with composition close to ideal stoichiometry found near Biancavilla (Catania, Sicily, Italy) lead us to study this unusual occurrence and to examine in detail the crystal structure combining single-crystal X-ray diffraction (SCXRD) and electron microprobe chemical analysis (EMPA) and measuring H, Li, and F content by Secondary Ion Mass Spectrometry (SIMS). Infrared spectroscopy (FTIR) on single crystals was performed also, to check qualitatively the OH content. In addition, this study aims at giving a contribution on the stability fields of the fluoro-phases, already found in the volcanic products of Biancavilla, and to provide further information for both petrologic and environmental health considerations. For comparative purposes a fluorophlogopite (labeled F_{syn}) synthesized following the procedure in Hammouda et al. (1995) and structurally characterized by us, is also considered here.

The sample used in this work has been recognized as the fluorophlogopite holotype by IMA-CNMMN (2006-011). It is held permanently at the Museo di Mineralogia, Dipartimento di Scienze della Terra, Università degli Studi di Roma "La Sapienza," Italy with code 33003/1.

Occurrence

Fluorophlogopite has been found in locally metasomatized benmoreitic autoclastic lavas at Biancavilla (Catania, Mount Etna, Sicily). These volcanic products are reported as "autoclastic breccias" in the geo-volcanological study of Etna Volcano, by Romano (1982). Fluorophlogopite crystals occur within interstitial, friable altered material in lava fissures and breccias and have been observed as very thin, flat laminae with a diameter of 200–400 μm. Fluorophlogopite is primarily associated with fluoro-edenite, alkali-feldspars, clino- and ortho-pyroxenes, fluorapatite, hematite, and pseudobrookite. The genetic process involved F- and Cl-rich fluids, which locally metasomatized the benmoreite lava body and allowed crystallization of this peculiar mineral assemblage.

Physical and optical properties

Fluorophlogopite is pale yellow and is transparent and non-fluorescent with vitreous to resinous luster; it shows yellowish-white color in thin section. Mohs' hardness is 2–3, and it is brittle and malleable. There is a perfect cleavage on {001}. The calculated densities using both the empirical formula and single-crystal data, and empirical formula and powder data are quite similar, i.e., 2.830 and 2.842 g/cm^3, respectively.

The fluorophlogopite is optically biaxial (–), $n_{\alpha calc} = 1.5430(8)$, $n_\beta = 1.5682(5)$, $n_\gamma = 1.5688(5)$ (immersion and wavelength variation methods; $\lambda = 589$ nm), $2V_{x(meas.)} = 17(2)°$ (Tobi's method) with $X \perp (001)$. There is no visible pleochroism.

Chemical composition

Major-element composition of the crystals used for crystal structure refinement was obtained with a Cameca SX-50 electron microprobe at the Istituto di Geologia Ambientale e Geoingegneria (IGAG), Università di Roma "La Sapienza." Analytical conditions were 15 kV accelerating voltage, 15 nA beam current, and 10 µm beam size. Counting times were 10 s for backgrounds and 20 s for peaks, except F and Cl (40 s) and Na (10 s). The following standards were employed: jadeite (Na), periclase (Mg), wollastonite (Si and Ca), rutile (Ti), corundum (Al), magnetite (Fe), metallic manganese (Mn), metallic chromium (Cr), orthoclase (K), barite (Ba), synthetic fluorphlogopite (F), and sylvite (Cl). A conversion from X-ray counts to oxide weight percentages (wt%) was obtained with the PAP data reduction method (Pouchou and Pichoir 1985).

Analysis of minor elements (H, Li) was performed by Secondary Ion Mass Spectrometry (SIMS) measurements on the same mount used for EMPA investigations of the natural fluorophlogopite. Previous studies showed that F content from EMPA is generally underestimated (Ottolini et al. 2000; Mesto et al. 2006). Therefore, F concentration was obtained by SIMS with a CAMECA IMS 4f ion microprobe installed at CNR-IGG, Pavia (Italy), and used for the final formula recalculation. Details about experimental conditions and data analysis are described in Mesto et al. (2006). The sample mounts were then re-polished smoothly, carbon coated and investigated at the electron microprobe proxy to the SIMS craters. These EMPA data were then used in the final SIMS quantification procedure with Si as the inner reference element.

The averaged results of EMPA (over 6 spots) and SIMS (over 2 spots) analysis and the derived atoms per formula units apfu are listed in Table 1. For comparison the chemical analysis and the derived atoms per formula unit of a synthetic sample (Hammouda et al. 1995) are given in Table 1.

Infrared spectroscopy

Transmission micro-FTIR unpolarized spectra (Fig. 1) were collected, in the range 4000–750 cm^{-1}, on the same natural single crystal used for crystal structure refinement using a Nicolet 380 with Continuum microscope, equipped with a MCT-A nitrogen-cooled detector and a KBr beam splitter. Nominal resolution was 4 cm^{-1} and the final spectrum was the average of 200 scans.

X-ray analysis

Powder X-ray diffraction data in the 2θ range 5–80° (Table 2) were obtained with a Gandolfi camera (114.6 diameter) operating at 40 kV and 20 mA with Ni-filtered Cu$K\alpha$ radiation on a single crystal of about 150 µm diameter. Unit-cell parameters and standard errors were calculated using the Appleman and Evans indexing program (Appleman and Evans 1973).

Single-crystal X-ray data collection was performed by means of a Bruker AXS X8 APEX automated diffractometer equipped with a four-circle Kappa goniometer and a CCD detector with a maximum active area of 62 mm^2, under monochromatized Mo$K\alpha$ radiation with 512 × 512 pixels resolution. Three sets of 12 frames were used for the initial unit-cell determination, each frame measured with 0.5° phi rotation and 10 s exposure time. The crystal-to-detector distance was 40 mm, and the collection strategy was optimized by the Apex program suite (Bruker 2003a). The complete data collection was accomplished by several ω and φ rotation sets with 0.5° scan width and 10 s per frame exposure time. The whole Ewald sphere ($\pm h$, $\pm k$, $\pm l$) was recorded in the range $2 < \theta < 40°$. A total of 18 644 and 22 118 reflections, in almost the same θ range, were collected respectively for the natural and synthetic sample. A semi-empirical absorption correction based on the intensities of equivalent reflections was applied by means the SADABS software (Sheldrick 2003), and the data were corrected for Lorentz, polarization and background effects. The package SAINT-IRIX (Bruker 2003b) was employed for data reduction and unit-cell refinement.

Structure refinement

Anisotropic structure refinements based both on F_o and F_o^2 were carried out in space group $C2/m$ using a recent version of

TABLE 1. Average chemical composition from EMPA and SIMS data, and structural formulas for the crystal studied here (F_{nat}) and the synthetic phase (F_{syn})

	F_{nat}		F_{syn}
Oxides (wt%)			
SiO_2	45.75(39)		43.37
Al_2O_3	9.60(19)		12.10
MgO	27.92(30)		28.96
FeO	1.25(6)		0.01
TiO_2	1.05(5)		–
MnO	0.16(3)		–
K_2O	8.22(11)		11.37
Na_2O	0.61(30)		0.02
BaO	0.09(5)		–
Li_2O*	0.30(1)		–
F	8.09(22)		9.02
F*	8.69(24)		–
Cl	0.02(1)		–
H_2O*	0.16(2)		–
Total	103.81		104.85
O = F,Cl	–3.67		–3.90
Total	100.14		100.95
Atoms per formula unit based on 12 (O, OH, F, Cl)			
	F_{nat}†	F_{nat}‡	
Si	3.163(13)	3.154(12)	3.01
Al	0.782(14)	0.780(13)	0.99
ΣT	3.945	3.934	4
Mg	2.878(23)	2.869(20)	3.00
Fe^{2+}/Fe^{3+}	0.072(4)	0.072(4)	–
Ti	0.055(3)	0.054(3)	–
Li	0.083(4)	0.080(4)	–
Mn	0.009(2)	0.009(2)	
ΣOct.	3.097	3.084	3.00
K	0.725(9)	0.723(8)	1.01
Na	0.082(40)	0.082(40)	–
Ba	0.002(1)	0.002(1)	–
ΣInt.	0.809	0.807	1.01
F	1.899(50)	1.910(50)	1.98
Cl	0.002(1)	0.003(1)	–
OH	**0.074(8)**	**0.071(8)**	**0.02**
ΣA	1.975	1.984	2

Notes: Standard deviations are given in parentheses. T = Tetrahedral; Oct. = Octahedral; Int. = Interlayer; A = Anion.
* Formulae calculated with H_2O*, Li_2O*, F* from SIMS data.
† F_{nat} calculated assuming $X_{Fe^{2+}} = 1$.
‡ F_{nat} calculated assuming $X_{Fe^{3+}} = 1$; see text for details.

the program CRYSTALS (Betteridge et al. 2003) starting from the data of Hazen and Burnham (1973). Reflections with $I > 3\sigma(I)$ were considered as observed during the structure refinement. Full occupancy of Mg was assigned at M1 and M2 sites, except for M2 site of F_{nat}, where mixed occupancies of Mg and Fe were refined. Scattering curves for fully ionized chemical species were used for non-tetrahedral sites, whereas ionized vs. neutral scattering curves were used for Si and O (Hawthorne et al. 1995). Refined parameters were: scale factors, atomic positions, cation occupancy and atomic displacement factors. The relevant agreement indexes were: $R = 4.40$, $R_w = 5.40$, $R_{sym} = 3.72\%$ for the natural fluorophlogopite and $R = 3.16$, $R_w = 3.73$, $R_{sym} = 3.06\%$ for the synthetic fluorophlogopite. Analysis of the 0*kl* and 1*kl* synthetic precession images obtained from the collected images of the natural fluorophlogopite showed diffuse streaks parallel to **c*** for $k \neq 3n$ reflections. Diffuse $k \neq 3n$ reflections coexisting with sharp $k = 3n$ family reflections are a well-known feature in micas, being indicative of stacking disorder. Difference-Fourier maps revealed some residual electron density peaks located at positions corresponding to the interlayer and tetrahedral sites shifted with respect to the basic structure by $\pm b/3$ along [010], [310], and [3$\bar{1}$0]. Therefore, two different scale factors (0.479, 0.521) were refined for the family and the non-family reflections (Nespolo and Ferraris 2001). At the end of this second anisotropic refinement (R = 3.50, R_w = 4.37%), the spurious peaks were no longer present in the difference-Fourier map. Crystal data, data-collection parameters, and some details concerning the structure refinement of the samples investigated here are reported in Table 3. Final atomic coordinates, occupancies and anisotropic and equivalent isotropic displacement parameters are given in Table 4. Selected interatomic bond distances in Å are listed in Table 5, whereas the distortion parameters commonly used in crystal chemical studies on micas are reported in Table 6. Finally, mean atomic numbers for F_{nat} and F_{syn} as obtained from structure refinement are compared to those calculated from chemical analyses in Table 7.

TABLE 2. X-ray Cu*K*α powder diffraction data (Gandolfi camera) for fluorophlogopite from Biancavilla, Etna Sicily, Italy

$I_{(estim.)}$*	$I_{(calc)}$	d_{meas}	d_{calc}	*h k l*
80	100	9.99	9.99	0 0 1
30	3	4.97	4.99	0 0 2
	14		4.60	0 2 0
70	20	4.57	4.54	1 1 0
20	6	4.41	4.40	$\bar{1}$ 1 1
30	19	3.91	3.92	1 1 1
70	55	3.63	3.65	1 1 $\bar{2}$
10	81	3.37	3.38	0 2 2
10	60	3.32	3.33	0 0 3
80	80	3.12	3.13	1 1 2
50	55	2.90	2.90	1 1–3
20	27	2.69	2.70	0 2 3
	37	2.61	2.61	2 0 0
80	73		2.61	$\bar{1}$ 3 1
20	5	2.50	2.50	0 0 4
	24	2.43	2.43	2 0 1
80	48		2.43	1 3 $\bar{2}$
20	12	2.29	2.29	$\bar{2}$ 2 1
70	39	2.16	2.17	$\bar{1}$ 3 3
	20		2.17	2 0 2
20	4	2.09	2.09	0 4 2
70	20	1.995	1.998	0 0 5
20	5	1.902	1.901	1 3 $\bar{4}$
	2		1.901	2 0 3
10	2	1.820	1.824	$\bar{2}$ 2 4
80	42	1.663	1.666	$\bar{1}$ 3 5
	21		1.666	2 0 4
20	10	1.637	1.641	$\bar{3}$ 1 3
	6		1.641	3 1 1
20	7	1.607	1.610	$\bar{2}$ 4 3
	10		1.610	1 5 2
20	6	1.574	1.576	$\bar{1}$ 5 3
	8		1.576	2 4 2
80	44	1.532	1.532	$\bar{3}$ 3 1
	22		1.533	0 6 0
30	5	1.513	1.515	$\bar{3}$ 3 2
	5		1.515	3 3 0
	5		1.515	0 6 1
20	3	1.467	1.468	$\bar{1}$ 3 6
	1		1.468	2 0 5
20	2	1.427	1.427	0 0 7
20	4	1.397	1.399	2 2 5
	10	1.354	1.356	$\bar{2}$ 0 7
70	21		1.356	1 3 6
30	8	1.320	1.322	$\bar{4}$ 0 2
	15		1.322	2 6 0
40	6	1.304	1.306	$\bar{3}$ 3 5
	6		1.306	3 3 3
	6		1.306	0 6 4
	2		1.306	1 1 7
	2		**1.268**	**4 0 1**
10	**5**	**1.269**	**1.268**	**2 6 $\bar{3}$**

Note: For comparison intensity data calculated by PowderCell (Nolze and Kraus 1998) are given.
* Visual estimation.

RESULTS AND DISCUSSION

Chemical data (Table 1) show the natural fluorophlogopite composition to be similar to the synthetic fluorophlogopite one. Main differences are relevant to Si, Al, and K content, occurrence of Fe, Ti, Li, Na, and traces of Mn. SIMS measurements allow to make an accurate estimate of the atomic fluorine fraction $X_F = 0.95$ [$X_F = F/(F + OH + O)$], thus confirming the end-member character of phlogopite from Biancavilla.

The vibrational spectrum of fluoropholgopite in the range 1250–750 cm^{-1} (Fig. 1) exhibits two characteristic strong absorption bands (Jenkins 1989). The band at 1155 cm^{-1} is due to Si-O stretching vibrations while the band at 837 cm^{-1} is directly related to stretching vibrations involving tetrahedral Al content.

TABLE 3. Refined cell parameters and data-collection parameters for the F_{nat} and F_{syn} samples studied by single-crystal XRD

Sample name	F_{nat}	F_{syn}
Crystal dimensions (mm)	0.300 × 0.166 × 0.015	0.475 × 0.390 × 0.010
Crystal system	Monoclinic	Monoclinic
Space group	*C*2/*m*	*C*2/*m*
Unit-cell dimensions		
a (Å)	5.3094(4)	5.3167(2)
b (Å)	9.1933(7)	9.2123(3)
c (Å)	10.1437(8)	10.1534(3)
β (°)	100.062(5)	100.105(2)
Volume (Å^3)	487.51(7)	489.59
θ range for data collection (°)	2 to 40	2 to 42
Index range	$-9 \le h \le 9$	$-9 \le h \le 9$
	$-16 \le k \le 16$	$-14 \le k \le 17$
	$-18 \le l \le 18$	$-18 \le l \le 18$
Reflections collected/	18644/	22118/
Unique/*R* merging [$R_{(int)}$] (%)	1607/3.72	1742/3.06
Reflections used	**728 with** $I > 3\sigma(I)$	910 with $I > 3\sigma(I)$
No. of refined parameters	**69**	**67**
GooF*	**0.830**	**0.900**
R_1† (on *F*)/wR_2‡ (on F^2)	0.0350/0.086	0.0316/0.071
$(\Delta/\sigma)_{max}$	0.022	0.036
$\Delta\rho_{min}/\Delta\rho_{max}$ (e/Å^3)	–0.23/0.53	–0.22/0.38

* GooF = $|\Sigma|w(F_o^2 - F_c^2)^2|/(n - p)|^{1/2}$, where *n* is the number of reflections and *p* is the total number of parameters refined.
† $R_1 = \Sigma||F_o| - |F_c||/\Sigma|F_o|$.
‡ $wR_2 = \{\Sigma[w(F_o^2 - F_c^2)^2]/\Sigma[w(F_o^2)^2]\}^{1/2}$.

TABLE 4. Atomic coordinates and displacement parameters of the studied micas (F_{nat} and F_{syn})

Atom	*x*	*y*	*z*	Occupancy	U_{iso}	U_{11}	U_{22}	U_{33}	U_{12}	U_{13}	U_{23}
Sample F_{nat}											
K	0	0	0	0.8662(8)	0.0324	0.0300(7)	0.0324(8)	0.0347(8)	0	0.0054(6)	0
T [Si]	0.5751(1)	0.1666(1)	0.2251(1)	0.9897(10)	0.0105	0.0087(2)	0.0090(2)	0.0142(3)	0.0000(3)	0.0026(2)	0.0001(2)
M1 [Mg]	0	0.5	0.5	0.9793(9)	0.0116	0.0090(6)	0.0082(7)	0.0182(8)	0	0.0039(5)	0
M2 [Mg]	0	0.8335(1)	0.5	0.9814(8)	0.0124	0.0082(4)	0.0124(5)	0.0169(5)	0	0.0032(3)	0
M2 [Fe]	0	0.8335(1)	0.5	0.0185(7)	0.0124	0.0082(4)	0.0124(5)	0.0169(5)	0	0.0032(3)	0
O1	0.8182(3)	0.2369(2)	0.1662(2)	1.0000(8)	0.0206	0.0182(7)	0.025(1)	0.0187(8)	–0.0006(7)	0.0039(6)	–0.0067(7)
O2	0.5293(5)	0	0.1665(3)	1.0001(8)	0.0207	0.030(1)	0.014(1)	0.018(1)	0	0.002 (1)	0
O3	0.6303(3)	0.1668(2)	0.3905(2)	1.0001(8)	0.0110	0.0094(5)	0.0097(6)	0.0142(6)	–0.0002(6)	0.0028(4)	0.0003(6)
F	0.1332(3)	0	0.4017(2)	0.9969(9)	0.0137	0.0120(7)	0.0121(8)	0.0173(9)	0	0.0035(6)	0
Sample F_{syn}											
K	0	0	0	1.0079(7)	0.0322	0.0325(5)	0.0337(5)	0.0301(5)	0	0.0051(4)	0
T [Si]	0.5753(1)	0.1666(1)	0.2251(1)	0.9871(9)	0.0108	0.0099(2)	0.0104(2)	0.0123(2)	0.0001(2)	0.0023(1)	0.0002(2)
M1 [Mg]	0	0.5	0.5	1.0000(6)	0.0106	0.0092(4)	0.0098(5)	0.0129(5)	0	0.0021(4)	0
M2 [Mg]	0	0.8309(1)	0.5	0.9992(7)	0.0107	0.0094(3)	0.0099(3)	0.0130(3)	0	0.0021(2)	0
O1	0.8220(2)	0.2341(2)	0.1668(1)	1.0003(8)	0.0187	0.0176(5)	0.0234(6)	0.0155(5)	–0.0022(5)	0.0038(4)	–0.0057(5)
O2	0.5239(4)	0	0.1667(2)	1.0006(8)	0.0187	0.0241(8)	0.0146(7)	0.0165(8)	0	0.0010(7)	0
O3	0.6305(2)	0.1663(1)	0.3905(1)	0.9997(8)	0.0105	0.0102(4)	0.0103(4)	0.0111(4)	–0.0005(4)	0.0019(3)	0.0000(4)
F	0.1329(3)	0	0.4026(2)	1.0008(7)	0.0128	0.0112(6)	0.0122(6)	0.0152(6)	0	0.0030(5)	0

Notes: Standard deviations are given in parentheses. The cations used for occupancy refinement are quoted in square brackets.

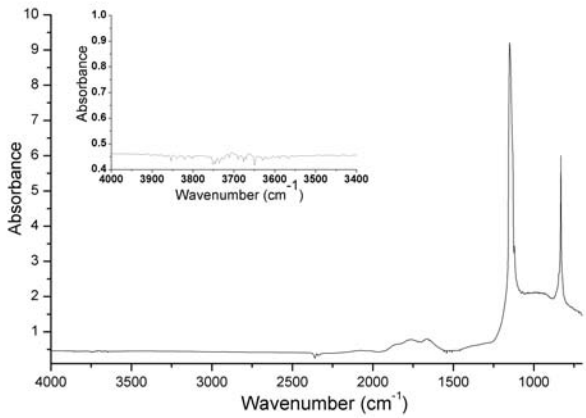

FIGURE 1. IR spectrum obtained by transmission-method on the same crystal of fluorophlogopite from Biancavilla used for single-crystal X-ray analysis, in the range 750–4000. The region 3400–4000 cm^{-1} is enlarged in the inset.

TABLE 5. Selected bond distances (Å)

	F_{nat}	F_{syn}
T-O1	1.646(2)	1.652(1)
T-O1′	1.649(2)	1.650(1)
T-O2	1.646(1)	1.651(1)
T-O3	1.652(2)	1.654(1)
<T-O>	1.648(2)	1.652(1)
M1-F (×2)	2.027(2)	2.027(1)
M1-O3 (×4)	2.082(2)	2.082(1)
<M1-O>	2.064(2)	2.064(1)
M2-F (×2)	2.021(2)	2.037(1)
M2-O3 (×2)	2.081(2)	2.071(1)
M2-O3′ (×2)	2.080(1)	2.081(1)
<M2-O>	2.061(2)	2.063(1)
<M-O>	2.062(2)	2.063(1)
K-O1 (×4)	3.014(2)	2.996(1)
K-O1′ (×4)	3.248(2)	3.284(1)
K-O2 (×2)	3.015(3)	2.995(2)
K-O2′ (×2)	3.251(3)	3.282(2)
$<K-O>_{inner}$	3.014(3)	2.996(1)
$<K-O>_{outer}$	3.249(3)	3.283(1)
<K-O>	**3.132(3)**	**3.140(1)**

Note: Standard deviations are given in parentheses.

The spectrum (Fig. 1) did not show any relevant OH-absorption band in the region 3800–3600 cm^{-1}, giving further support to the chemical results.

Structural details

Structural details from refinement are indicative of the end-member fluorophlogopite . The refined unit-cell parameters from X-ray powder-diffraction data for F_{nat} [a = 5.305(2), b = 9.189(3), c = 10.137(4) Å, β = 100.02(3)°] agree with those obtained by single-crystal X-ray studies (Table 3).

These values are close to the corresponding values of fluorophlogopites reported in literature (see Table 8). The c cell parameter [10.1437(8) Å] is significantly shorter than that in OH-phlogopite [10.310(6) Å, Redhammer and Roth 2002]. Because F-OH substitution changes the H^+-K^+ coulombic repulsion into F^--K^+ attraction, the interlayer separation decreases from about 3.487 Å in the end-member OH-phlogopite (Redhammer and Roth 2002) to 3.322 Å (this study), reducing the c repeat distance and cell volume remarkably. The a and b parameters of F_{nat} are similar to the observed values for end-member OH-phlogopite (Redhammer and Roth 2002), F-rich Franklin phlogopite (Hazen and Burnham 1973), and synthetic fluorophlogopites (see Table 8), being determined essentially by the Mg content of the octahedral sheet (for more details see below in this section).

The tetrahedron in F_{nat} is fairly regular and slightly elongated along the T-O_{apical} bond distance (O_{basal}-T-O_{apical} = 110.89°, O_{basal}-T-O_{basal} = 108.23°). The tetrahedral bond lengths T-O1, T-O2 for both F_{nat} and F_{syn} are within one standard deviation (Table 5). In fluorophlogopite, the mean bond length <T-O> is significantly shorter, 1.648(2) Å (Table 5), than that in OH-phlogopite, 1.658(1) Å (Table 9), owing to Si/Al ratio >> 3. This observation is consistent with the IR spectrum, in particular the 1250–750 cm^{-1} spectral region (see Fig. 1). The band at 1155 cm^{-1}, due to Si-O stretching vibrations, is shifted toward higher wavenumbers compared to that in the OH-phlogopite (995 cm^{-1} in Jenkins 1989). The tetrahedron in synthetic fluorophlogopite is slightly more regular. In fact it is characterized by bond length distortion (BLD) and tetrahedral angle variation (TAV) values lower than

TABLE 6. Selected distortion parameters

	F_{nat}	F_{syn}
t_{tet} (Å)	2.239	2.236
BLD_T	0.142	0.079
V_T (Å^3)	2.30	2.31
TQE	1.0007	1.0005
TAV	2.680	2.012
τ (°)	110.89	110.68
α (°)	5.17	6.31
Δz (Å)	0.003	–0.001
D.M. (Å)	0.487	0.514
Ψ_{M1} (°)	59.20	59.28
Ψ_{M2} (°)	59.16	59.26
BLD_{M1}	1.174	1.180
ELD_{M1}	5.364	5.457
BLD_{M2}	1.280	0.835
ELD_{M2}	5.304	5.427
$Shift_{M2}$ (Å)	0.0016	–0.0022
V_{M1} (Å)	11.49	11.49
OQE_{M1}	1.013	1.014
OAV_{M1}	42.066	43.917
V_{M2} (Å^3)	11.44	11.47
OQE_{M2}	1.013	1.014
OAV_{M2}	41.666	44.571
e_uM1 (Å)	3.070	3.073
e_sM1 (Å)	2.757	2.755
e_uM2 (Å)	3.064	3.071
e_sM2 (Å)	2.756	2.755
t_{oct} (Å)	2.113	2.108
t_{int} (Å)	3.322	3.334
$\Delta_{K\text{-}O}$ (Å)	0.235	0.287
$t_{K\text{-}O4}$ (Å)	**3.950**	**3.963**

Notes: t_{tet} = tetrahedral sheet thickness calculated from z coordinates of basal and apical O atoms; TQE = tetrahedral quadratic elongation calculated as TQE = $\Sigma_i(l_i/l_0)^2/4$ where l_0 is the center to vertex distance for an undistorted tetrahedron (Robinson et al. 1971); TAV = $\Sigma_i(\theta_i - 109.47°)^2/5$ (Robinson et al. 1971); τ = tetrahedral flattening angle; α = tetrahedral rotation angle (Hazen and Burnham 1973); Δz = departure from co-planarity of the basal O atoms, calculated as Δz = $(z_{o2} - z_{o1})c\sin\beta$ (Güven 1971); D.M. = dimensional misfit between tetrahedral and octahedral sheets defined as D.M. = $[2\sqrt{3}\ \langle O\text{-}O\rangle_{bas} - 3\sqrt{2}\ \langle M\text{-}O\rangle]$ (Toraya 1981); ψ = octahedral flattening angles (Donnay et al. 1964); BLD = $100/n \times \Sigma_i |(M\text{-}O)_i - \langle M\text{-}O\rangle|/\langle M\text{-}O\rangle$ (Renner and Lehmann 1986); ELD = $100/n \times \Sigma_i |(O\text{-}O)_i - \langle O\text{-}O\rangle|/\langle O\text{-}O\rangle$ (Renner and Lehmann 1986); $Shift_{M2}$ = off-center shift of the M2 cation defined as the distance between the refined position of cation and the geometrical center of M2 site (coordinates: x/a = 0.0, y/b = 0.8333, z/c = 0.5); OQE = octahedral quadratic elongation calculated as OQE = $\Sigma_i(l_i/l_0)^2/6$ where l_0 is the center to vertex distance for an undistorted octahedron (Robinson et al. 1971); OAV = $\Sigma_i(\theta_i - 90°)^2/11$ (Robinson et al. 1971); e_u,e_s = mean lengths of unshared and shared edges (Toraya 1981), respectively; t_{oct} = octahedral sheet thickness (Toraya 1981); t_{int} = calculated from the z coordinates of basal O atoms; $\Delta_{K\text{-}O} = \langle K\text{-}O\rangle_{outer} - \langle K\text{-}O\rangle_{inner}$; $t_{K\text{-}O4}$ = projection of K-O4 distance along **c***.

in natural fluorophlogopite (see Table 6). The slightly longer <T-O> mean distance in synthetic fluorophlogopite with respect to the natural analogue [1.652(1) vs. 1.648(2) Å] is consistent with the different Si content (3.01 vs. 3.16 apfu).

The main tetrahedral distortion parameters commonly considered in micas are the in-plane rotation angle (α), the thickening angle (τ), and the basal corrugation (Δz). The rotation angle is known to be a function of tetrahedral and octahedral sheet compositions and is the most effective mechanism to obtain congruence between tetrahedral and octahedral sheet sizes. The crystal structure of the natural fluorophlogopite of this study showed a small rotation angle (α_{nat} = 5.17°), which is in good agreement with the calculated value (α_{calc} = 4.60°) based on the geometrical model of Brigatti and Guggenheim (2002). In particular, $\alpha_{calc} = \arccos[(3/4)^{1/2}k]$, where k is the ratio between the $\langle O\text{-}O\rangle_u$ unshared octahedral edges and $\langle O\text{-}O\rangle_b$ tetrahedral basal edges. Note that α decreases as $\langle O\text{-}O\rangle_u$ increases and $\langle O\text{-}O\rangle_b$ decreases; the latter mechanism is observed in this case. The mean basal tetrahedral edge depends on tetrahedral cation content ($\langle O\text{-}O\rangle_{bsyn}$ = 2.675 Å vs. $\langle O\text{-}O\rangle_{bnat}$ = 2.665 Å) and influences the ditrigonal distortion parameter α (α_{syn} = 6.31° vs. α_{nat} = 5.17°) and the potassium-oxygen distances ($\Delta K\text{-}O_{syn}$ = 0.287 Å vs. $\Delta K\text{-}O_{nat}$ = 0.235 Å).

The high value (11.4) of the effective coordination number (ECoN), calculated through the iterative procedure described in Nespolo et al. (2001), is consistent with the low α value (α = 5.17°) and with the small difference (ΔK-O = 0.235 Å) between the inner and outer potassium-oxygen distances (McCauley and Newnham 1971; Weiss et al. 1992).

The angle τ is a measure of the distortion of the tetrahedra by elongation or compression normal to the sheet. This angle changes with Si content, tetrahedral cation position and mean value of basal oxygen distance bonds. The measured τ angle of F_{nat} (110.89°) is greater than the ideal tetrahedral angle [arcos (–1/3) = 109.47°] and indicates tetrahedra elongated in T-O apical direction. The τ values found in natural and synthetic fluorophlogopite are consistent with the short $\langle O\text{-}O\rangle_b$ bond distance and the Si atoms per formula unit (Brigatti and Guggenheim 2002).

The Δz parameter is strongly related to differences in octahedral sizes (Brigatti and Guggenheim 2002): $\Delta M = \langle M\text{-}O\rangle_{max} - \langle M\text{-}O\rangle_{min}$ (ΔM_{nat} = 0.003 Å, ΔM_{syn} = 0.001 Å). In synthetic fluorophlogopite this value, negligible within the experimental errors, confirms the homo-octahedral (Ďurovič 1981, 1994) character of the F_{syn}. This is also reflected in an almost ideal value of the interlayer shift (–0.3338 *a*) according to Drits et al. (1984). Natural fluorophlogopite, F_{nat}, exhibits small but significantly differences with respect to F_{syn} when the values of M-O, T-O individual distances and mean atomic numbers (m.a.n. values) are compared (see Tables 5 and 7). These mirror the slight compositional difference existing between the two samples (see Table 1). However, we observe that M1 sites of F_{nat} and F_{syn} are characterized by similar values of M1-O individual bond distances, volume, BLD_{M1}, ELD_{M1}, and Ψ_{M1} (see Tables 5 and 6), pointing to the same site composition. By contrast the small differences between M2 sites (compare M2-O individual distances, m.a.n. values, BLD_{M2}, $shift_{M2}$; Tables 5, 6, and 7), indicate that other cations besides Mg (probably Ti and Li as discussed later) occupy the M2 site. This is further supported by the analysis of equivalent displacement parameters of M1 and M2 sites of F_{nat}

TABLE 7. Mean atomic numbers (m.a.n. values, e$^-$) of cation sites, octahedral and tetrahedral mean distances (Å), as determined by structure refinement (X-ref) and chemical determinations (EMPA)—see text for details

	F_{nat}	F_{syn}
$e^-_{(M1+M2)X\text{-}ref}$	36.27(7)	35.98(3)
$e^-_{(M1+M2)EMPA}$	36.00	36.00
$e^-_{(M1)X\text{-}ref}$	11.75(1)	12.00(1)
$e^-_{(M1)EMPA}$	11.73	12.00
$e^-_{(M2)X\text{-}ref}$	12.26(3)	11.99(1)
$e^-_{(M2)EMPA}$	12.14	12.00
$K\,e^-_{X\text{-}ref}$	16.46(2)	19.15(1)
$K\,e^-_{EMPA}$	14.83	19.02
$T\,e^-_{X\text{-}ref}$	13.86(1)	13.82(1)
$T\,e^-_{EMPA}$	14.02	13.75
Σ^+	21.94	22.02
Σ^-	22.03	22.00
$\langle T\text{-}O\rangle_{X\text{-}ref}$	1.648(2)	1.652(1)
$\langle T\text{-}O\rangle_{EMPA}$	1.654	1.657
$\langle M\text{-}O\rangle_{X\text{-}ref}$	2.062(2)	2.063(1)
$\langle M\text{-}O\rangle_{EMPA}$	2.073	2.073

TABLE 8. Unit-cell parameters and composition of phlogopite and fluorophlogopite samples reported in the literature

Sample	*a* (Å)	*b* (Å)	*c* (Å)	β (°)	Crystal-chemical formula
Takeda and Donnay (1966)	5.31	9.21	10.13	100.01	$K_{0.95}Mg_{2.80}Li_{0.20}Si_{3.25}A_{0.75}O_{10}F_2$
Joswig (1972)	5.3141(11)	9.2024(5)	10.1645(7)	100.05(1)	$(K_{1.80}Na_{0.04})(Mg_{5.41}Fe^{2+}_{0.32}Al_{0.15}Ti_{0.06})(Si_{5.82}Al_{2.18})O_{19.80}(OH_{1.94}F_{2.26})$
McCauley et al. (1973)	5.308(2)	9.183(3)	10.139(1)	100.07(2)	$(K_{0.98}Na_{0.04})(Mg_{2.97})(Si_{2.98}Al_{1.02})O_{9.90}(OH_{0.16}F_{1.94})$
Hazen and Burnham (1973)	5.3078(4)	9.1901(5)	10.1547(8)	100.08(1)	$(K_{0.77}Na_{0.16}Ba_{0.05})(Mg_{3.00})(Si_{2.95}Al_{1.05})O_{10.00}(OH_{0.70}F_{1.30})$
Takeda and Morosin (1975)	5.3074(6)	9.195(2)	10.134(1)	100.08(1)	$K_1Mg_3Si_3Al_1O_{10}F_2$
Toraya et al. (1978)	5.292(1)	9.164(5)	10.143(1)	100.07(2)	$K_1Mg_{2.75}Si_{3.5}Al_{0.5}O_{10}F_2$
Toraya et al. (1983)	5.285(1)	9.157(1)	10.190(2)	99.97(2)	$K_1Mg_{2.44}Mn_{0.24}Si_{3.82}Mn_{0.18}O_{10}F_2$
Russell and Guggenheim (1999)	5.3346(7)	9.2417(8)	10.182(2)	100.26(1)	$(K_{1.85}Na_{0.16})(Mg_{3.14}Fe^{2+}_{2.13}Fe^{3+}_{0.21}Ti_{0.21}Mn_{0.12}\square_{0.19})(Si_{5.94}Al_{2.01}Ti_{0.05})O_{20.00}(OH_{2.10}F_{1.88}Cl_{0.02})$
Redhammer and Roth (2002)	5.3158(24)	9.2036(34)	10.3100(57)	99.891(59)	$K_1Mg_3Si_3Al_1O_{10}OH_2$
F_{nat} (this work)	5.3094(4)	9.1933(7)	10.1437(8)	100.062(5)	$(K_{0.72}Na_{0.08}Li_{0.01})(Mg_{2.87}Li_{0.07}Ti_{0.05}Mn_{0.01})(Si_{3.15}Al_{0.78}Fe^{3+}_{0.07})O_{10.03}(OH_{0.07}F_{1.90})$
F_{syn} (this work)	5.3167(2)	9.2123(3)	10.1534(3)	100.105(2)	$(K_{1.01})(Mg_{3.00})(Si_{3.01}Al_{0.99})O_{10.00}(OH_{0.02}F_{1.98})$

Note: Standard deviations are given in parentheses.

TABLE 9. Main structural parameters and selected mean interatomic distances of phlogopite and fluorophlogopite samples reported in the literature

	Takeda and Donnay 1966	Joswig 1972	McCauley et al. 1973	Hazen and Burnham 1973	Takeda and Morosin 1975	Toraya et al. 1978	Toraya et al. 1983	Russell and Guggenheim 1999	Redhammer and Roth 2002
t_{tet} (Å)	2.237	2.235	2.212	2.225	2.239	2.219	2.209	2.228	2.235
V_T (Å^3)	2.31	2.32	2.27	2.30	2.31	2.25	2.23	2.30	2.34
τ (°)	110.62	110.57	110.100	110.49	110.72	111.15	111.23	110.71	110.70
α (°)	6.21	7.69	5.88	7.54	6.50	3.63	1.73	4.29	9.20
D.M. (Å)	0.517	0.532	0.483	0.515	0.526	0.432	0.376	0.422	0.531
Ψ_{M1} (°)	59.35	59.20	59.00	59.00	59.36	58.79	58.36	58.66	58.76
Ψ_{M2} (°)	59.32	59.14	59.05	59.03	59.39	58.81	58.35	58.53	58.73
V_{M1} (Å^3)	11.44	11.53	11.475	11.50	11.349	11.51	11.687	11.99	11.71
V_{M2} (Å^3)	11.41	11.479	11.515	11.52	11.367	11.52	11.679	11.87	11.69
t_{oct} (Å)	2.102	2.116	2.124	2.125	2.095	2.137	2.172	2.174	2.152
t_{int} (Å)	3.328	3.356	3.356	3.352	3.329	3.334	3.372	3.344	3.488
<T-O> (Å)	1.650	1.654	1.642	1.649	1.651	1.638	1.632	1.650	1.658
<M-O> (Å)	2.060	2.064	2.063	2.064	2.071	2.063	2.070	2.085	2.073
$<K-O>_{inner}$ (Å)	2.995	2.970	3.006	2.969	2.987	3.045	3.096	3.051	2.973
$<K-O>_{outer}$ (Å)	3.278	3.319	3.273	3.312	3.282	3.209	3.174	3.247	3.389
Δ_{K-O} (Å)	0.283	0.351	0.267	0.343	0.295	0.164	0.078	0.196	0.416

if compared with those shown for F_{syn} (Table 4), which suggests a degree of chemical disorder at M2 site in F_{nat}.

It has already been stressed (see Introduction) that one of the most important factors determining the extent of halogen replacement of OH in micas is the cation population of octahedral sheet. Table 8 lists some F-rich phlogopites and fluorophlogopites that are characterized by different tetrahedral and octahedral site population. For comparison an OH-phlogopite is also included. Table 9 illustrates some distortional parameters commonly used to compare structural features in micas. From the analysis of Tables 8 and 9 it can be seen that *c* unit-cell parameter ranges from 10.13 to 10.19 Å. Focusing our attention on the fluorophlogopites, it can be noted that the α value varies from 1.73 to 6.50°, independently of the F content. A comparison between the F- and OH-end-member shows a difference of about 3° in α values (Tables 8 and 9). This suggests that the F-OH substitution has a role in reducing the misfit between T-O sheets. Conversely, an octahedral site population that increases the sheets misfit favors the entrance of F into the structure to reduce the misfit (Munoz 1984). Finally we observed that two structural effects occur in F-OH substitution: the first one increases the octahedral angle ψ (ψ = 59.3 and 58.7° in F_{syn} and OH-phlogopite, respectively), see Tables 8 and 9; the second one shrinks the octahedral sheet due to the shortening of the octahedral cation-anion distances. The combination of both effects produces no substantial variation in *a* and *b* parameters as documented in Table 8. It follows that the main contribution to the α value is from tetrahedral sheet rotation produced by the substitution F for OH occurring in the octahedral sheet (cf. V_T and α of F_{syn} and OH-phlogopite in Tables 6 and 9). It is known that the substitution F for OH has important consequences on physico-chemical behavior of phlogopite (McCauley et al. 1973). On the basis of the results of this work [compare our data in Table 6 with those quoted in Table 9 for both Takeda and Morosin (1975) and Redhammer and Roth (2002)] this may due to two main reasons: (1) the structure becomes more compact as a consequence of the reduction of the *c* parameter due to the substitution of the attractive K-F for the repulsive K-H effect, and (2) the α value decreases reducing the trigonalization of T sheet and so causing an increase in the effective coordination around K. Note that $<K-O>_{inner}$ distance increases by 0.014 Å, while $<K-O>_{outer}$ decreases by 0.107 Å in F_{syn} (see Table 9), which enhances the structural stability.

Crystal-chemistry

Formula recalculation is not a trivial task in micas and should be carefully checked by comparison among independent techniques, such as SCXRD and, when possible, spectroscopic or other methods (see Cruciani 1993 and Waters and Charnley 2002, for a review). In particular, a direct knowledge of the light elements content seems to be a fundamental step to assess the correct substitutional mechanisms in micas (Cesare et al. 2003; Mesto et al. 2006).

The calculation of the crystal chemical formula of natural fluorophlogopite given in Table 1 was performed by combining EMPA with SIMS determinations for Li, H, and F. Regarding Fe, no experimental evidences of its valence state are available

to date because the paucity of the sample and the low concentration of Fe in fluorophlogopite prevented the use of Mössbauer spectroscopy. A tentative crystal-chemical formula was obtained on the basis of 12 (O, OH, F, Cl) and assuming all Fe as Fe^{2+} and Ti as Ti^{4+} (see Table 1). It turned out that the tetrahedral site was not completely filled [Si + Al < 4 apfu], whereas five cations (Li, Mg, Fe, Ti, Mn) overpopulated the octahedral sheet [octahedral site closure >3 apfu]; OH and F anions summed to ~2 apfu. It was concluded that (1) Ti or Fe must populate the tetrahedral site to obtain full occupancy; (2) the oxy-component is negligible, or even absent within 1σ (see Table 1); and (3) no octahedral vacancies occur.

Points 2 and 3 above indicate that, in the case here, Ti uptake into the mica structure does not occur via $2^{VI}R^{2+} \leftrightarrow {}^{VI}Ti^{4+} + {}^{VI}\square$ (Ti-vacancy substitution) and $^{VI}R^{2+} + 2(OH)^- \leftrightarrow {}^{VI}Ti^{4+} + 2O^{2-} + H_2$ (Ti-oxy substitution). Accordingly, a structural formula consistent with EPMA, SIMS and the results of structural refinement is:

$$(K_{0.73}Na_{0.08}Li_{0.04})_{\Sigma 0.85}(Mg_{2.88}Fe^{2+}_{0.07}\ Li_{0.04}Mn_{0.01})_{\Sigma 3.00}(Si_{3.16}Al_{0.78}Ti_{0.06})_{\Sigma 4.00}O_{10.03}(OH_{0.07}F_{1.90}) \quad (1)$$

The assignment of Ti^{4+} at tetrahedral site in formula 1 satisfies the full occupancy of the tetrahedral site improving the agreement between the refined site-scattering value and that calculated from the electron-microprobe analyses: 13.93 vs. 13.86 m.a.n. values. A good agreement is also found between observed (from X-ray refinement) and calculated (from molar fractions and radii in Shannon 1976) mean <T-O> distances, 1.648(2) and 1.653 Å, respectively.

Lithium was distributed over interlayer and octahedral sites so that the remaining cations (Mg, Fe, Mn) with part of Li completely populate the octahedral sheet. This partition provides a good agreement between m.a.n. values obtained from the refined scattering powers and the ones calculated from chemical analysis: 36.27 vs. 36.75 e^-. However, formula 1 proved to be unsatisfactory because it was not possible to work out substitution mechanisms commonly active in micas. In addition, the following reasons led us to question the initial assumption that all Fe was Fe^{2+}: (1) Mössbauer spectroscopy performed on the host rock showed primarily Fe^{3+} (G. Andreozzi, private communication); (2) the associated minerals (in particular hematite and pseudobrookite) contain only Fe^{3+}; (3) fluorescence is absent (see physical and optical properties section). Based on the above considerations we propose two more crystal chemical formulae:

$$(K_{0.72}Na_{0.08}Li_{0.03})_{\Sigma 0.83}(Mg_{2.87}Fe^{3+}_{0.07}\ Li_{0.05}Mn_{0.01})_{\Sigma 3.00}(Si_{3.15}Al_{0.78}Ti_{0.05})_{\Sigma 3.98}O_{10.03}(OH_{0.07}F_{1.90}) \quad (2)$$

$$(K_{0.72}Na_{0.08}Li_{0.01})_{\Sigma 0.81}(Mg_{2.87}Ti_{0.05}Li_{0.07}Mn_{0.01})_{\Sigma 3.00}(Si_{3.15}Al_{0.78}Fe^{3+}_{0.07})_{\Sigma 4.00}O_{10.03}(OH_{0.07}F_{1.90}). \quad (3)$$

Formula 3 is more reliable on the basis of points 1 to 3 mentioned above, and of the local charge balance principle. It is easily seen, indeed, that (1) trivalent cations in tetrahedral site equilibrate almost entirely the interlayer charge, and (2) ^{VI}Ti is engaged into two substitution mechanisms. More precisely, 0.02 Ti apfu are balanced through $^{VI}R^{2+} + 2^{IV}Si^{4+} \leftrightarrow {}^{VI}Ti^{4+} + 2^{IV}Al^{3+}$ (Ti-Tschermak substitution), whereas 0.03 Ti apfu balance 0.06 Li apfu through the mechanism $2^{VI}Li + {}^{VI}Ti \leftrightarrow 3^{VI}Mg$.

At a short-range order level an equal partition of Li at M1 and M2 contiguous sites around Ti (in M2) seems electrostatically favored. Finally, we observe the average octahedral radius that can be obtained from the cation distribution at M1 ($Mg_{0.970}Li_{0.030}$) and at M2 ($Mg_{0.950}Li_{0.020}Mn_{0.005}Ti_{0.025}$) using Shannon's (1976) radii, is $\langle r\rangle_{M1} = \langle r\rangle_{M2} = 0.72$ Å, thus explaining the identical <M1-O> and <M2-O> distances, within 1σ, for F_{nat} (see Table 5).

Concluding remarks

From a geo-volcanological point of view, the finding of the fluorophlogopite in the volcanic rocks of Biancavilla is further evidence that metasomatic processes affected the pre-existing benmoreitic rocks of the Etnean volcanic area. The presence of the fluorophlogopite in association with the fluoro-edenite is also consistent with this hypothesis. The composition, structure, and crystal-chemistry of the fluorophlogopite would indicate a thermodynamic condition with high f_{O_2} during crystallization; indeed, all Fe is oxidized to Fe^{3+} and the other associated minerals contain mainly ferric iron. Moreover, it was possible to establish that in the fluorophlogopite from Biancavilla the Fe^{3+} prefers tetrahedral rather than octahedral coordination, involving a series of mechanisms that counterbalance lithium and Ti^{4+}. Finally, the particular anhydrous mineralogical assemblage (ortho- and clino-pyroxenes, alkali-feldspars, fluoro-edenite, fluorapatite, hematite, and pseudobrookite) shows that the fluorophlogopite crystallized under extremely very low P_{H_2O} conditions.

Acknowledgments

The authors are grateful to M. Serracino for assistance during electron probe microanalyses at the IGAG, Istituto di Geologia Ambientale e Geoingegneria, CNR, Rome. Special thanks go to A. Marconi, who spotted and supplied the first laminae of fluorophlogopite from Biancavilla. We thank G. Ferraris, M.F. Brigatti, J.B. Thompson, and the Associate Editor W.C. Elliott for their remarks and suggestions that allowed improving appreciably the manuscript. This work was supported by grants from the Italian MUR (Ministero dell'Università e della Ricerca).

References cited

Appleman, D.E. and Evans, H.T. Jr. (1973) Job 9214: Indexing and least-squares refinement of powder diffraction data. U.S. National Technical Information Service, Document PB 216 188.

Betteridge, P.W., Carruthers, J.R., Cooper, R.I., Prout, K., and Watkin, D.J. (2003) Crystals version 12: software for guided crystal structure analysis. Journal of Applied Crystallography, 36, 1487.

Bloss, F.D., Gibbs, G.V., and Cummings, D. (1963) Polymorphism and twinning in synthetic fluorophlogopite. Journal of Geology, 71, 537–547.

Boukili, B., Robert, J.L., Beny, J.M., and Holtz, F. (2001) Structural effects of OH → F substitution in trioctahedral micas of the system: K_2O-FeO-Fe_2O_3-Al_2O_3-SiO_2-H_2O-HF. Schweizerische Mineralogische und Petrographische Mitteilungen, 81, 55–67.

Boukili, B., Holtz, F., Bény, J.M., and Robert, J.L. (2002) Fe-F and Al-F avoidance rule in ferrous-aluminous (OH,F) biotites. Schweizerische Mineralogische und Petrographische Mitteilungen, 82, 549–559.

Brigatti, M.F. and Guggenheim, S. (2002) Mica crystal chemistry and the influence of pressure, temperature, and solid solution on atomistic models. In A. Mottana, F.P. Sassi, J.B. Thompson, and S. Guggenheim, Eds., Micas: Crystal Chemistry and Metamorphic Petrology, 46, p. 1–100. Reviews in Mineralogy and Geochemistry, Mineralogical Society of America, Chantilly, Virginia.

Bruker (2003a) APEX2. Bruker AXS Inc., Madison, Wisconsin.

——— (2003b) SAINT-IRIX. Bruker AXS Inc., Madison, Wisconsin.

Cesare, B., Cruciani, G., and Russo, U. (2003) Hydrogen deficiency in Ti-rich biotite from anatectic metapelites (El Joyazo, SE Spain): Crystal-chemical aspects and implications for high-temperature petrogenesis. American Mineralogist, 88, 583–595.

Comba, P., Gianfagna, A., and Paoletti, L. (2003) The pleural mesothelioma cases in Biancavilla are related to the new fibrous amphibole fluoro-edenite. Archives of Environmental Health, 58, 4, 229–232.

Cruciani, G. (1993) Studio di cristallochimica comparativa su flogopiti 1*M* naturali, 154 p. Ph.D. thesis, University of Perugia, Italy.

Donnay, G., Donnay, J.D.H., and Takeda, H. (1964) Trioctahedral one-layer micas. II. Prediction of the structure from composition and cell dimensions. Acta Crystallographica, 17, 1374–1381.

Drits, V.A., Plançon, A., Sakharov, B.A., Besson, G., Tsipursky, S.I., and Tchoubar, C. (1984) Diffraction effects calculated for structural models of K-saturated montmorillonite containing different types of defects. Clay Minerals, 19, 541–561.

Ďurovič, S. (1981) OD-Charakter, Polytypie und Identifikation von Schichtsilikaten. Fortschritte der Minerogie, 59, 191–226.

——— (1994) Classification of phyllosilicates according to the symmetry of their octahedral sheets. Ceramics-Silikaty, 38, 81–84.

Fechtelkord, M., Behrens, H., Holtz, F., Bretherton, J.L., Fyfe, C.A., Groat, L.A., and Raudsepp, M. (2003) Influence of F content on the composition of Al-rich synthetic phlogopite: Part II. Probing the structural arrangement of aluminum in tetrahedral and octahedral layers by ^{27}Al MQMAS and ^{1}H/^{19}F-^{27}Al HETCOR and REDOR experiments. American Mineralogist, 88, 1046–1054.

Gianfagna, A. and Oberti, R. (2001) Fluoro-edenite from Biancavilla (Catania, Sicily, Italy): Crystal chemistry of a new amphibole end-member. American Mineralogist, 86, 1489–1493.

Gianfagna, A., Ballirano, P., Bellatreccia, F., Bruni, B., Paletti, L., and Oberti, R. (2003) Characterization of amphibole fibres linked to mesothelioma in the area of Biancavilla, Easthern Sicily, Italy. Mineralogical Magazine, 67(6), 1221–1229.

Güven, N. (1971) The crystal structure of 2*M*1 phengite and 2*M*1 muscovite. Zeitschrift für Kristallographie, 134, 196–212.

Hammouda, T., Pichavant, M., Barbey, P., and Brearley, A.J. (1995). Synthesis of fluorphlogopite single crystals. European Journal of Mineralogy, 7, 1381–1387.

Hawthorne, F.C., Ungaretti, L., and Oberti, R. (1995) Site populations in minerals: terminology and presentation of results. Canadian Mineralogist, 33, 907–911.

Hazen, R.M. and Burnham, C.W. (1973) The crystal structure of one layer phlogopite and annite. American Mineralogist, 58, 889–900.

Jenkins, D.M. (1989) Empirical study of the infrared lattice vibrations (1100–350 cm^{-1}) of phlogopite. Physics and Chemistry of Minerals, 16, 408–414.

Joswig, V.W. (1972) Neutronenbeugungsmessungen an einem 1*M*-phlogopit. Neues Jahrbuch für Mineralogie, Monatshefte, 1–11.

Mason, R.A. (1992) Models of order and iron-fluorine avoidance in biotite. Canadian Mineralogist, 30, 343–354.

McCauley, J.W. and Newnham, R.E. (1971) Origin and prediction of ditrigonal distorsions in micas. American Mineralogist, 56, 1626–1638.

McCauley, J.W., Newnham, R.E., and Gibbs, G.V. (1973) Crystal structure analysis of synthetic fluorophlogopite. American Mineralogist, 58, 249–254.

Mesto, E., Schingaro, E., Scordari, F., and Ottolini, L. (2006) An electron microprobe analysis, secondary ion mass spectrometry, and single-crystal X-ray diffraction study of phlogopites from Mt. Vulture, Potenza, Italy: Consideration of cation partitioning. American Mineralogist, 91, 182–190.

Munoz, J.L. (1984) F-OH and Cl-OH exchange in micas with application to hydrothermal deposits. In S.W. Bailey, Ed., Micas, 13, p. 469–493. Reviews in Mineralogy, Mineralogical Society of America, Chantilly, Virginia.

Nespolo, M. and Ferraris, G. (2001) Effects of the stacking faults on the calculated electron density of mica polytypes—the Durovic effect. European Journal of Mineralogy, 13, 1035–1045.

Nespolo, M., Ferraris, G., Ivaldi, G., and Hoppe, R. (2001) Charge distribution as a tool to investigate structural details. II. Extension to hydrogen bonds, distorted and hetero-ligand polyhedra. Acta Crystallographica, B57, 652–664.

Nolze, G. and Kraus, W. (1998) PowderCell 2.0 for Windows. Powder Diffraction, 13, 256–259.

Ottolini, L., Camara, F., and Bigi, S. (2000) An investigation of matrix effects in the analysis of fluorine in humite-group minerals by EMPA, SIMS, and SREF. American Mineralogist, 85, 89–102.

Papin, A., Sergent, J., and Robert, J-L. (1997) Intersite OH-F distribution in an Al-rich phlogopite. European Journal of Mineralogy, 9, 501–508.

Petersen, E.U., Essene, E.J., Peacor, D.R., and Valley, J.W. (1982) Fluorine end-member micas and amphiboles. American Mineralogist, 67, 538–544.

Pouchou, J-L. and Pichoir, F. (1985) 'PAP' F(r Z) procedure for improved quantitative micro-analysis. Microbean Analysis, 104–160.

Redhammer, G.J. and Roth, G. (2002) Single-crystal structure refinements and crystal chemistry of synthetic trioctahedral micas $KM_3(Al^{3+},Si^{4+})_4O_{10}(OH)_2$, where M = Ni^{2+}, Mg^{2+}, Co^{2+}, Fe^{2+}, or Al^{3+}. American Mineralogist, 87, 1464–1476.

Renner, B. and Lehmann, G. (1986) Correlation of angular and bond length distortions in TO_4 units in crystals. Zeitschrift für Kristallographie, 175, 43–59.

Robert, J-L., Beny, J-M., Della Ventura, G., and Hardy, M. (1993) Fluorine in micas: crystal-chemical control of the OH-F distribution between trioctahedral and dioctahedral sites. European Journal of Mineralogy, 5, 7–18.

Robinson, K., Gibbs, G.V., and Ribbe, P.H. (1971) Quadratic elongation, a quantitative measure of distortion in coordination polyhedra. Science, 172, 567–570.

Romano, R. (1982) Succession of the volcanic activity in the Etnean area. Memorie della Società Geologica Italiana, 23, 27–48.

Russell, R.L. and Guggenheim, S. (1999) Crystal structure of near-end-member phlogopite at high temperature and heat treated Fe-rich phlogopite: the influence of the O, OH, F site. Canadian Mineralogist, 37, 711–720.

Shannon, R.D. (1976) Revised effective ionic radii and systematic studies of interatomic distances in halides and chalcogenides. Acta Crystallographica, A32, 751–767.

Sheldrick, G.M. (2003) SADABS. University of Göttingen, Germany.

Shen, G., Lu, Q., and Xu, J. (2000) Fluorannite: A new mineral of mica group from Western suburb of Suzhou City. Acta Petrologica et Mineralogica, 19, 63–71.

Takeda, H. and Donnay, J.D.H. (1966) Trioctahedral one-layer micas. III. Crystal structure of a synthetic Lithium Fluormica. Acta Crystallographica, 20, 638–646.

Takeda, H. and Morosin, B. (1975) Comparison of observed and predicted structural parameters of mica at high temperature. Acta Crystallographica, B31, 2444–2452.

Toraya, H. (1981) Distortions of octahedra and octahedral sheets in 1*M* micas and the relation to their stability. Zeitschrift für Kristallographie, 157, 173–190.

Toraya, H., Iwai, S., and Marumo, F. (1978) The crystal structure of synthetic mica, $KMg_{2.75}Si_{3.5}Al_{0.5}O_{10}F_2$. Mineralogical Journal, 9, 210–220.

Toraya, H., Marumo, F., and Hirao, M. (1983) Synthesis and the crystal structure of a mangaoan fluoromica, $KMg_{2.14}Mn_{0.24}Si_{3.82}Mn_{0.18}O_{10}F_2$. Mineralogical Journal, 11, 240–247.

Waters, D.J. and Charnley, N.R. (2002) Local equilibrium in polymetamorphic gneiss and the titanium substitution in biotite. American Mineralogist, 87, 383–396.

Weiss, Z., Rieder, M., and Chmielovà, M. (1992) Deformation of coordination polyhedra and their sheets in phyllosilicates. European Journal of Mineralogy, 4, 665–682.

Xu, J. and Shen, G. (2005) Mineralogical study on fluorphlogopite from the Bayan Obo ore deposit. Kuangwu Xuebao, 25(3), 213–216.

Manuscript received November 8, 2006
Manuscript accepted May 28, 2007
Manuscript handled by W. Crawford Elliott